ARCHIVES OF ACOUSTICS
12, 3–4, 311–318 (1987)

AN ARRAY RECEIVER SCHEME FOR REDUCING REFRACTION INDUCED ARTIFACTS IN ULTRASONIC TOF TOMOGRAPHY

K. SRINIVASA RAO, T. M. SRINIVASAN

Indian Institute of Technology
(Madras 600 036, India)

Different types of errors caused by refraction effects in ultrasonic time-of-flight (TOF) tomography are discussed. The effectiveness of a three element experimental array receiver in reducing refraction induced artifacts in ultrasonic TOF tomography is evaluated. During data acquisition, TOF and peak values of the received signal is measured for each of the three receivers. A peak value index (PVI) is computed for each receiver. The PVIs give an indication of the deviation of the interrogating beam from line-of-sight path. Based on these indices a propagation path is assumed for the ultrasonic beam in the medium and image reconstruction is performed along these assumed propagation paths. These propagation paths are closer to the actual paths than the generally assumed line-of-sight paths and hence superior tomograms are obtained when reconstruction is done along these assumed propagation paths. Tomograms of agar gel objects and excited sheep heart indicate that this method is effective in reducing the geometric distortions in the reconstructions. The tomograms are quantitatively evaluated using two error measures.

1. Introduction

In ultrasonic time-of-flight (TOF) tomography, refraction effects give rise to inaccurate reconstructions, poor resolution and geometric degradations [5]. The origin of these errors can be traced back to the data acquisition schemes used in ultrasonic tomography. Following the conventional X-ray tomography techniques, in ultrasonic tomography a finite aperture receiver is placed opposite to the transmitter along the line-of-sight. However, due to refraction, an ultrasound beam launched at the transmitter, does not travel strictly along the line-of-sight path in the medium. Due to this, a portion of the transmitted beam may fail to reach the finite aperture receiver, thus causing a reduction in the amplitude of the received signal. In TOF tomography, due to time-walk and time-hop phenomenon, variations in received signal amplitude cause errors in estimation of time of flight [6]. Particularly, when the beam is incident upon the boundary of a curved refractive structure, deviation from straight line path is large and time-walk and time-hop errors will be predominant. When these erroneous TOF projections measured over

non-straight line paths are processed with standard straight line reconstruction methods, the quantitative accuracy of the tomograms will further deteriorate.

The finite width of the transmitted beam, refraction and diffraction effects give rise to multiple propagation paths between the transmitter and the receiver [9]. Under multipath conditions the TOF measuring circuit always registers the TOF of the first arriving pulse. Because of this the TOF tomograms show poor resolution and macrostructural geometric degradations [5]. The nature of these geometric degradations is such that regions of higher acoustic speed appear larger and regions of lower acoustic speed appear smaller than their geometric sizes. It has been demonstrated that the magnitude of these geometric degradations are refraction dependent. Multipath also gives rise to errors in TOF estimates. When multiple rays arrive at the receiver at different time instants, there will be phase cancellation effects [5]. This will appear as noise in TOF projection data.

Resolution in TOF tomography depends upon the speed of ultrasound within a resolution cell. For example, very small regions of high acoustic speed will cause some energy to arrive earlier than the bulk of energy through different pathways and hence such regions can be easily detected [8]. Conversely, in case of small regions of low acoustic speed, the energy received from these regions will be masked by the bulk of energy arriving earlier through paths having higher acoustic speed. This masking will occur even if the bulk of the energy is arriving through regions of low acoustic speed. Thus the resolution is poor for regions of low acoustic speed.

Attempts have been made to compensate for refraction effects in velocity tomograms [1, 3, 5]. These are post-reconstructive cleaning up procedures and are iterative in nature. These methods have provided only modest improvement in the image quality, but the resolution is not improved [9]. Moreover, it is preferable to prevent the refraction induced artifacts from entering into the reconstructions rather than trying to refine the corrupted tomograms. A method based on this approach is experimentally investigated and reported in the present work.

In the method presented here, an array receiver is used. By using an array receiver with sufficiently large aperture, artifacts caused by the parts of beam missing the receiver can be reduced [2]. By measuring the signal on each element of the array, beam profile at the receiving plane can be obtained and depending upon the location of the peak amplitude point of the beam profile, a propagation path can be assumed for the interrogating beam through the medium. As a first step in implementing the array receiver system, three closely spaced individual hydrophones are used. The three transducers are placed opposite to the transmitter such that the central receiver is in line with the transmitter as shown in Fig. 1. The line which joins the center of the transmitter with the transducer registering maximum acoustic field amplitude is selected as the propagation path of the ultrasound in the medium. Since usually these assumed propagation paths are closer to the actual in comparison to the generally assumed straight line paths, images of more accurate dimensions are obtained by reconstructing along these paths.

2. Method

Each hydrophone of the receiving array has a 2 MHz PZT element of 2 mm diameter. The center-to-center spacing between the hydrophones is 4 mm. The transmitter consists of a 2 MHz PZT element of 20 mm diameter. During data acquisition, at each step, the TOF and the peak value of the received signal is measured for each of the three hydrophones. The TOF is measured with a resolution of 1 ns and the peak value is measured with 8 bits resolution. A microprocessor controlled data acquisition system is used to acquire the projection data. Thirty projections are measured from the object with an angular spacing of 6° between the projections and the linear sampling interval for each projection is 2 mm. At the end of the experiment, the measured projection data is transferred to a remote image processing computer (PDP 11/23) through a RS 232C communication link.

For a straight line propagation path, the peak amplitude point of the ultrasound beam also shifts to one of the side receivers and the peak value measured from that peak value measured from this receiver will be relatively large. When the propagation path deviates from the straight line path, the peak amplitude point of the beam also shifts to one of the side receivers and the peak value measured from that side receiver will have a relatively larger value. Thus, the peak values measured from the receivers can be used to detect the deviation from the straight line path. In order to compensate for the unequal sensitivities of the receivers a peak value index (PVI) is defined as:

$$\text{peak value index (PVI)} = P_0/P_m, \tag{1}$$

where P_0 – peak value of the signal received with the object in the coupling medium between the transducers; P_m – peak value of the received signal with only the coupling medium between the transducers.

With a straight line propagation path, if the entire cross section of the beam is subjected to the same amount of attenuation, the peak value indices of all the receivers will be equal. When the propagation path is bent towards any of the off central receivers, the corresponding receiver will have a maximum value of PVI. It should be noted that the knowledge of maximum PVI for a given receiver will not provide precise information about the actual propagation path. However, as a first order approximation, the line joining the center of the transmitter and the receiver having maximum PVI is assumed to be the propagation path of the interrogating beam. The TOF recorded by that receiver having maximum PVI is back projected along this assumed propagation path. Since the signal amplitude on this receiver is large, the TOF measured from the receiver will be least affected by the time-walk and time-hop errors [6].

The standard reconstruction algorithms require equiangularly spaced projections measured over a straight line path. The three sets of TOF projections measured with

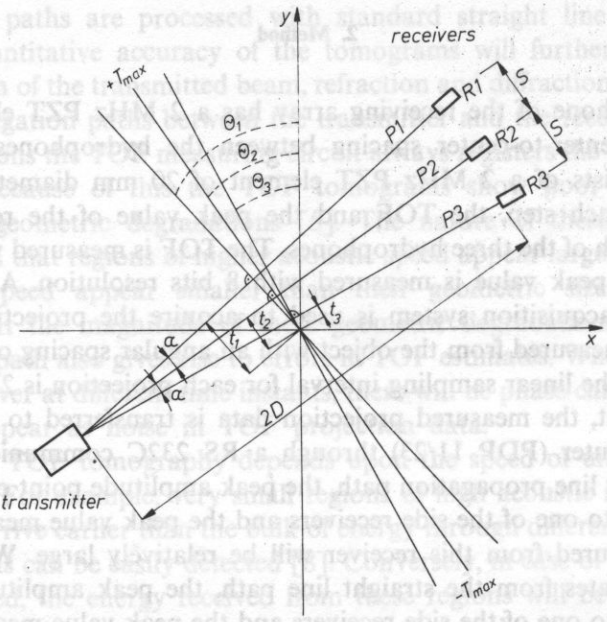

Fig. 1. Transducer configuration for three receiver technique

this three receiver scheme are rearranged using a sorting algorithm to obtain a single modified projection set so that standard reconstruction methods can be used. The sorting algorithm used here is the same as the one used to convert fan beam projections into parallel ray projections [7] and is based on the mathematical relation between the ray sums of the three receivers as given below.

The geometry of the scanning apparatus is shown in Fig. 1. Let the projections be denoted as $P(\Theta, t)$, where Θ and t define the propagation path of the interrogating beam. For the line integral measured over the propagation path $P2$ with the middle receiver $R2$, Θ is equal to Θ_2 and t is equal to t_2 as shown in Fig. 1. From the geometry it can be shown that for small values of α (in the present experimental setup $\alpha = 2°$ and $\cos\alpha$ is taken equal to unity) Θ and t corresponding to the propagation path $P1$ are given by

$$\Theta_1 = \Theta_2 + \alpha \quad \text{and} \quad t_1 = t_2 + S/2. \tag{2}$$

where S is the spacing between the receivers. Similarly, for propagation path $P3$, the corresponding relations are

$$\Theta_3 = \Theta_2 - \alpha \quad \text{and} \quad t_3 = t_2 - S/2. \tag{3}$$

It can be inferred from the above equations that the straight line propagation path $P2$ for a given Θ and t coincides with the propagation path $P1$ or $P3$ for appropriately modified values of Θ and t. Thus we may say that the line integrals measured by the receivers $R1$ or R3 are the same as the one that would be measured

by the middle receiver $R2$ for a suitably modified values of Θ and t. This fact is used in sorting the projection data. When the PVI of, say, receiver $R1$ is more than that of the other two receivers, the TOF by the central receiver $R2$ is ignored and the TOF measured by receiver $R1$ is placed in an appropriate location in the modified projections.

In order to simplify the sorting procedure, the TOF projections and the peak amplitude value projections measured at an angular spacing of 6° are expanded by first order interpolation to obtain projections at 2° spacing, so that the angular spacing is equal to α. The additional projection data thus generated by interpolation also reduces the noise in reconstructed images [7]. While sorting the projections at $\Theta = 2°$ and at $\Theta = 178°$ it is possible that they may give rise to entries in modified projections, at projection angles $\Theta = -2°$ and $\Theta = 180°$. The appropriate location of these values in final projection are selected based on criteria:

$$P(\Theta, t) = P(\Theta + 180, -t). \tag{4}$$

After the sorting is completed, it is found that in some of the locations of the modified projection set, there are no entries. This situation arises when the maximum value of PVI jumps from $R1$ to $R3$ or vice versa. However, the number of such locations is usually less than 10 percent of the total line integrals in the projection. The TOF values corresponding to these locations are computed from the TOF values of the neighbourhood locations, by using first order interpolation.

The conventional filtered back projection algorithm is used to reconstruct a 64×64 pixel image from these 90 modified projections. For comparison, an image is reconstructed from the 90 interpolated projections of the middle receiver alone. This image is the same as the one that would have been generated by a standard tomographic scanner employing a single receiver. For display purpose, these images are expanded by first order interpolation to 256×256 pixels.

3. Results and discussion

The merit of the three receiver technique is evaluated qualitatively using two different objects and quantitatively by two error coefficients namely, the geometric distortion coefficient and the normalized mean squared error. The geometric distortion coefficient δ [4] gives a measure of the macrostructural geometric degradations present in the reconstructions. This is measured by comparing the threshold versions of a reference tomogram and a test tomogram. Thresholding is done such that all pixels below a threshold are set to zero and all pixels above this value are set to one. If I and J are the reference and test tomograms after the above procedure, the distortion measure is given by

$$\delta = \frac{1}{N \cdot N} \sum_{i=1}^{N} \sum_{j=1}^{N} |I(i, j) - J(i, j)|, \tag{5}$$

where i, j are pixel co-ordinate and $N \times N$ is the image dimension. The standard normalised mean squared error (NMSE) [10] between the reference tomogram and the test tomogram is used as a measure of the quantitative accuracy.

To simplify the computation, the error coefficients are evaluated for tomograms of an agar gel cylinder. The tomogram of a cylinder is circular in shape and has a constant TOF value in all pixels. The error free projections of such cross section can be generated mathematically [10]. Tomograms reconstructed from these computed projections are used as reference tomograms for evaluating the error coefficients. The propagation velocity of ultrasound in agar gel is equal to that in water at room temperature. Hence, the refractive nature of the object is controlled by altering the temperature of water bath. Table 1 shows the error coefficients for tomograms of agar gel cylinder obtained at two different values of V_α which is the difference between the propagation velocity of ultrasound in the object and in the coupling medium. For evaluating the geometric distortion coefficient the threshold level is chosen as half the average TOF value across the cross section. It can be observed that the geometric distortion coefficients are less for the tomograms obtained with the proposed three receiver technique in comparison to those of the tomograms obtained using single receiver. The NMSE values are also less for the three receiver tomograms thus indicating that these TOF values are closer to the actual values for these objects.

The two objects used for qualitative evaluation are an agar gel cylinder with a hole (scanned in transformer oil $V_\alpha = 36$ m/s) and an excised sheep heart. TOF tomograms of these objects are shown in Fig. 2 and Fig. 3 respectively. The bright circles superimposed on the images in Fig. 2 represent the boundaries of the original object. The effectiveness of the proposed three receiver technique in reducing the geometric distortions is evident from the three receiver tomograms given in Fig. 2(b) and Fig. 3(b). It may be noticed that the geometric distortion in the tomograms is not eliminated completely. This is due to the limited number of elements in the

Table 1. Geometric distortion coefficient (δ) and normalised mean squared error NMSE for tomograms of an agar gel cylinder

Object	δ	NMSE
Agar gel cylinder $V_\alpha = 24$ m/s		
Single receiver	0.01928	0.0415
Three receivers	0.01733	0.0321
Agar gel cylinder $V_\alpha = -21$ m/s		
Single receiver	0.07885	0.1276
Three receivers	0.06543	0.0997

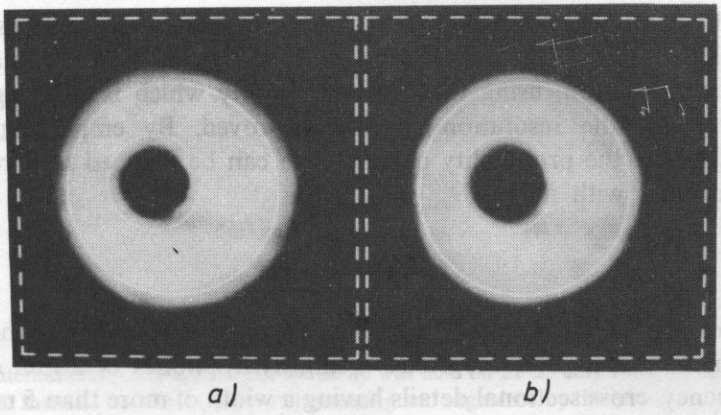

Fig. 2. TOF tomograms of an agar gel object scanned in transformer oil $V_\alpha = 36$ m/s (a) Tomogram obtained using a single receiver. (b) Tomogram obtained using three receivers

receiving array. By using an array with more number of elements the geometric distortion can be further reduced. In the three receiver tomogram of the excised sheep heart, though there is some improvement in the sizes of the left ventricle and that of the whole heart, the size of the right ventricle is reduced. This drawback arises from the fact that the PVI values can detect the deviation from straight line propagation path only if the entire cross section of the beam is subjected to the same amount of attenuation. In the actual sheep heart the width of the right ventricle is only about 5 mm, due to which the above assumption is invalidated. In this case also, by employing an array with more number of elements, actual beam profile in the receiving plane can be obtained and using this information, the deviation from straight line path can be detected with higher accuracy.

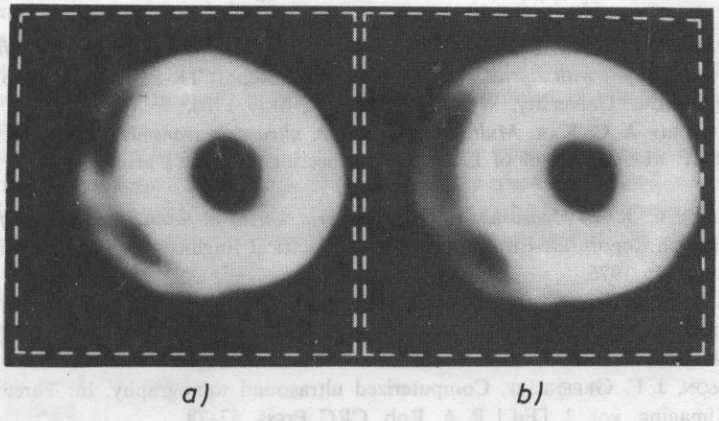

Fig. 3. TOF tomograms of an excised sheep heart. The circular hole is the left ventricle and the elongated hole is the right ventricle. (a) Tomogram obtained using single receiver. (b) Tomogram obtained using three receivers

As already mentioned, limited resolution of the TOF tomograms arises from the method employed for measuring TOF. Instead of using the TOF of first arriving ray for image reconstruction, using the TOF of the ray which is carrying maximum amount of energy the resolution can be improved. By employing a narrow interrogating beam, the probability of multipath can be reduced thus reducing the artifacts associated with it.

4. Conclusions

The three receiver array system used here is effective in reducing the geometric distortions in time-of-flight tomograms. Using hydrophones of 2 mm diameter at 2 MHz frequency, cross sectional details having a width of more than 5 mm could be improved. Details smaller than this dimension are not improved by this scheme. This is thought to be due to the limited number of elements in the receiving array. Optimization of number of receivers and frequency of operation is under progress. Better methods for measuring the TOF are being investigated.

References

[1] S. A. JOHNSON, J. F. GREENLEAF, W. F. SAMAYOA, F. A. DUCK, J. D. SJOSTRAND, *Reconstruction of three dimensional velocity fields and other parameters by acoustic ray tracing*, Ultrasonic Symp. Proc., IEE Cat. 75 CHO 994-3SU, 46–51 (1975).

[2] R. M. SCHMIDT, C. R. MEYER, P. L. CARSON, T. L. CHENVERT, P. H. BLAND, *Error reduction in through transmission tomography using large receiving arrays with phase insensitive signal processing*, IEEE Trans. on Sonics and Ultrasonics, SU-31, 4, 251–248 (1984).

[3] H. SCHOMBERG, *An improved approach to reconstructive ultrasound tomography*, J. Phys. D: Appl. Phys., **11**, 15, L181–L185 (1978).

[4] P. SOBEL, R. M. RANGAYYAN, R. GORDON, *Quantitative and qualitative evaluation of geometric deconvolution of distortion in limited-view computed tomography*, IEEE Trans. on Biomed. Eng., BME-32, 5, 330–335 (1985).

[5] A. H. ANDERSON, A. C. KAK, *The application of ray tracing towards a correction for refraction effects in computed tomography with diffracting sources*, Research Report TR-EE 84–14, School of Electrical Engineering, Purdue University, West Lafayette, IN, May 1984.

[6] C. R. CRAWFORD, A. C. KAK, *Multipath artifacts in ultrasonic transmission tomography*, Research Report TR-EE 81–43 School of Electrical Engineering, Purdue University, West Lafayette, IN, Dec. 1981

[7] K. A. DINES, A. C. KAK, *Measurement and reconstruction of ultrasonic parameters for diagnostic imaging*, Research Report TR-EE 77–4, School of Electrical Engineering, Purdue University, West Lafayette, In, Dec. 1976.

[8] J. F. GREENLAEF, S. A. JOHNSON, R. C. BAHN, B. RAJAGOPOLAN, S. KENUE, Introduction to computed ultrasound tomography, In: Computer aided tomography and ultrasonics in medicine [Eds.] Ravive et al. North-Holland Publ. Co. 1979, 125–136,

[9] B. S. ROBINSON, J. F. GREENLAEF, Computerized ultrasound tomography, In: Three dimensional biomedical imaging, vol. 2, [Ed.] R. A. Rob, CRC Press, 57–78.

[10] A. ROSENFIELD, A. C. KAK, Digital picture processing, vol. 1, Academic Press New York 1976.

Received on October 20, 1986.